This is a copy of the published version, or version of record, available on the publisher's website. This version does not track changes, errata, or withdrawals on the publisher's site.

Towards freeform reflective fused silica optics using ultrafast laser-assisted etching

Thibaud Van Gorp, Aurélien Benoît, Calum A. Ross, Pablo Roldán-Varona, Chris Evans, David Lee, Duncan P. Hand, Robert R. Thomson

Published version information:

Citation: Thibaud Van Gorp et al., Towards freeform reflective fused silica optics using ultrafast laser-assisted etching, Proceedings Volume 13100, Advances in Optical and Mechanical Technologies for Telescopes and Instrumentation VI; 131007A (2024)

DOI: https://doi.org/10.1117/12.3022721

Copyright 2024. Society of Photo-Optical Instrumentation Engineers (SPIE). One print or electronic copy may be made for personal use only. Systematic reproduction and distribution, duplication of any material in this publication for a fee or for commercial purposes, and modification of the contents of the publication are prohibited.

This version is made available in accordance with publisher policies. Please cite only the published version using the reference above. This is the citation assigned by the publisher at the time of issuing the APV. Please check the publisher's website for any updates.

This item was retrieved from **ePubs**, the Open Access archive of the Science and Technology Facilities Council, UK. Please contact epublications@stfc.ac.uk or go to http://epubs.stfc.ac.uk/ for further information and policies.

Towards Freeform Reflective Fused Silica Optics using Ultrafast Laser-Assisted Etching

Thibaud Van Gorp[a], Aurélien Benoît[a], Calum A. Ross[a], Pablo Roldán-Varona[a], Chris Evans[b], David Lee[c], Duncan P. Hand[a], and Robert R. Thomson[a]

[a]SUPA, Institute of Photonics and Quantum Sciences, Heriot-Watt University, Edinburgh EH14 4AS, UK

[b]European Space Agency (ESA), ESA Office, Space Telescope Science Institute, 3700 San Martin Drive, Baltimore, MD 21218, USA

[c]STFC UK Astronomy Technology Centre, Royal Observatory, Blackford Hill, Edinburgh EH9 3HJ, UK

ABSTRACT

While conventional methods like diamond turning can achieve the necessary precision for manufacturing image slicers, they are often expensive in cost and time, and restrictive in terms of the materials to which they can be readily applied. Ultrafast laser-assisted etching (ULAE) is an emerging manufacturing technology that could potentially be used to manufacture free form reflective optics using fused silica, as it enables µm-level precision shaping of fused silica over several millimetres scales. Here we demonstrate the potential of ULAE for manufacturing fused silica image slicers by fabricating precision 8×1 mm flat fused silica surfaces using ULAE. The waviness meets the required level for this application, staying below 1 µm. Specifically, we measured $S_{10z} = 0.164$ µm. The roughness varies with surface inclination; for a flat surface at $0°$ inclination, we measured $S_q = 109$ nm, while at a $5°$ inclination, it increased to $S_q = 204$ nm. If combined with a suitable polishing technique to remove the high spatial frequency roughness, we believe this work demonstrates that ULAE provides a new route to manufacture freeform reflective monolithic fused silica optics such as image slicers for ground- and space-based applications.

Keywords: Optical manufacturing, ultrafast-laser, chemical-etching, image-slicer

1. INTRODUCTION

Integral field spectroscopy enables spectrally resolved images of the night sky to be captured. This can be achieved using an image slicer, a technology introduced in 1938,[1] that can rearrange a two-dimensional field-of-view into longitudinally aligned strip to match a spectrograph entrance slit. This technology has become standard in many modern observatories, and several designs have emerged.[2,3] Most of them are manufactured using traditional methods, such as polishing and diamond turning.[4,5] Among them, the VLT-MUSE instrument, with its 24 integral-field units made up of 48 slices.[6] Its significant contributions to scientific exploration since its first light in March 2014 underscores the importance of image slicers in advanced astronomical instrumentation.[7,8] Despite being manufactured using refined traditional techniques aimed at reducing both time and cost,[9] its construction remained a labor-intensive process, demanding considerable effort and expertise.

An emergent technology that could enable the precision fabrication of image slicers is ultra fast-laser assisted etching (ULAE).[10–15] Unlike ablative laser machining, ULAE is a two-step process. In the first step, sub-bandgap ultrafast laser pulses are tightly focused into a dielectric material, such as fused silica, creating a modified region only at the focal volume position. Translating the sample through the focus allows 3D structural modifications to be inscribed with a sub-micron precision. If correctly controlled the material modification manifests itself through an increase in the chemical etching rate (ER) if exposed to a suitable solvent *e.g.*, KOH or NaOH. The material surrounding the laser modified material remains unaffected, and etching selectivities of 1:1000

E-mail: tv2012@hw.ac.uk

Advances in Optical and Mechanical Technologies for Telescopes and Instrumentation VI,
edited by Ramón Navarro, Ralf Jedamzik, Proc. of SPIE Vol. 13100, 131007A
© 2024 SPIE · 0277-786X · doi: 10.1117/12.3022721

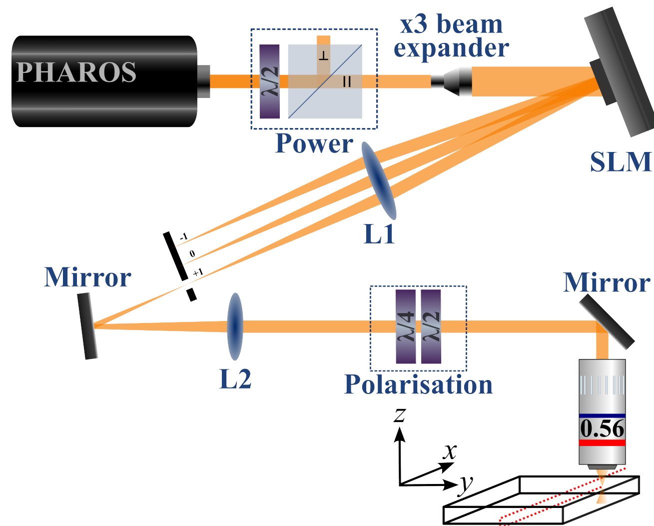

Figure 1. Schematic representation of the writing setup. A femtosecond laser generates ultrashort pulses. After a series of optics for power modulation and beam expansion, a spatial light modulator (SLM) is used to shape the laser beam phase and amplitude profile. The 1st order of the diffraction pattern passes through a 4-f system, quarter-wave plate and half-wave plate to control the final polarisation of the laser light that is focused into the fused silica substrate

between the pristine and modified material can be reached.[16] The surface quality after UALE, at both small and large spatial frequencies, roughness and waviness respectively, depends on the laser writing and chemical etching parameters.

For the image slicer application, the target waviness is below 1 µm peak-to-peak. The surface roughness directly following the etching ($S_q \approx 100 - 200$ nm RMS) will be too high for any optical reflective surface required to operate in the visible, which requires $S_q < 5$ nm RMS. However we aim to keep the S_q as low and consistent as possible to enable the easy application of post-process polishing method, such as CO_2 laser polishing.[17] In the first part of this paper, we present an optimisation of the writing parameters in order to build a repeatable protocol to fabricate precision surfaces. We develop optimised parameters to minimise the ultrafast laser writing time in order to reduce the impact of instabilities that could occur during the ultrafast laser writing process. In the second part of the paper, a method for characterizing the surface is presented. This allows fine-tuning of the inscription to achieve a fully controlled process in the design of free-form fused silica optics.

2. OPTIMISATION OF INSCRIPTION PARAMETERS FOR SELECTIVE CHEMICAL ETCHING

2.1 ULAE experimental methods

A schematic of the experimental setup for ultrafast laser inscription is shown in Fig. 1. The inscription was performed using an ultrafast laser emitting 370 fs laser pulses with a central wavelength of 1030 nm (Pharos, Light Conversion). A pulse picker enables the pulse repetition rate to be reduced from 1 MHz to the kHz regime while preserving the same individual pulse energy (E_p). Our inscription system also integrates a spatial light modulator (SLM) (X13138-08, Hamamatsu) to compensate for depth dependent aberrations. A 3× beam-expander was used to ensures the SLM aperture was filled (15.0 × 12.8 mm). For our purposes, the SLM was configured to diffract the laser beam into the 1st order, which was used for laser writing. This allowed both the shape and phase of the laser beam to be controlled. The beam then passed through a 4-f system and filled the entrance pupil of a long-working-distance objective (PAL-50-NIR-HR, OptoSigma) that focussed the beam with a numerical aperture of 0.56. A quarter-wave and half-wave plate were placed before the objective to control the writing polarisation. The sample translation was performed using a 3-axis air-bearing translation stage (ABL1000, Aerotech).

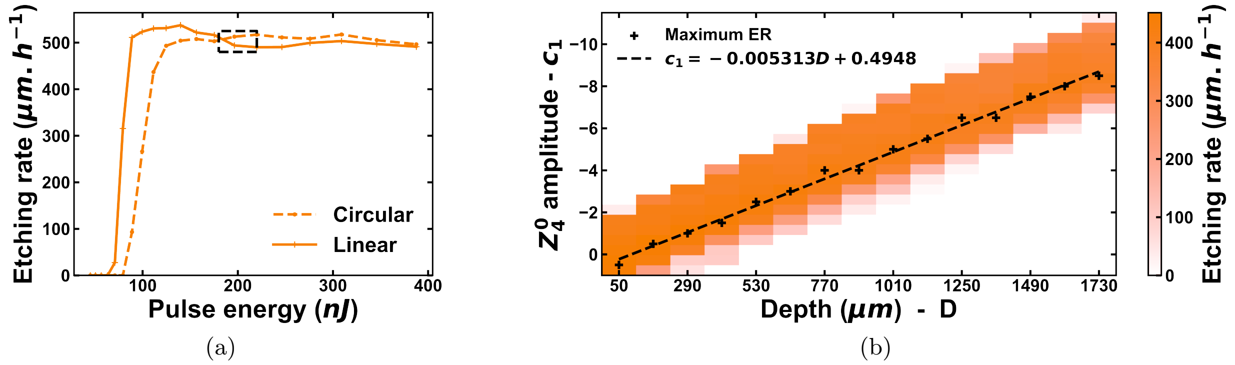

Figure 2. (a) Evolution of the etching rate as a function of pulse energy using either linear or circular polarisation, a translation speed of $4\,\mathrm{mm\,s^{-1}}$ and a pulse repetition rate of 15.6 kHz. (b) Evolution of the etching rate as a function of the writing depth and the Z_4^0 amplitude coefficients. A linear interpolation is used for continuous spherical aberration compensation.

After the inscription, samples are placed into a 5wt% NaOH solution[16] heated on by a hotplate to a temperature of $85 \pm 2\,^\circ\mathrm{C}$, for 180 min for the channel study. For individual slice fabrication, the etching time was minimised, and the samples were removed from the solution as soon as fully etched (≈90 min).

2.2 Optimisation of ULAE parameter for shallow structures

Preliminary investigations were aimed at maximising the etching rate of the laser modified material when inscribing structures at shallow depths within the substrate, where spherical aberration is expected to be minimal. To identify the optimal parameters, arrays of straight lines of modified material were inscribed at 100 µm depth, varying the pulse energy, pulse repetition rate, and substrate translation speed. Both circular and linear polarisations were tested, the orientation of the linear polarisation being perpendicular to the writing direction.[18] We investigated many parameter combinations, encompassing twenty E_p values ranging from 45 to 400 nJ (increasing in steps of +12% starting from the lowest pulse energy), eight pulse repetition rate values ranging from 1 MHz to 7.81 kHz (in steps of 2), and 4 translation speeds from 1 to $4\,\mathrm{mm\,s^{-1}}$ in step of $1\,\mathrm{mm\,s^{-1}}$. After inscription, the samples were polished on both edges to allow the etching solution to reach the modified region. Etching rates were measured using micrograph pictures.

Figure 2(a) presents the key results for the parameter optimization study, showing that etching rate of $400\,\mathrm{\mu m\,h^{-1}}$ can be achieved using a pulse energy higher than 150 nJ, a translation speed of $4\,\mathrm{mm\,s^{-1}}$ and a pulse repetition rate of 15.6 kHz. The etching rate was found to be independent of the laser polarisation, a property discovered recently for this writing regime.[19] Reducing the pulse energy towards the threshold was found to increase the sensitivity of etching rate to instabilities, such as fluctuations in laboratory temperature. For all further slice fabrication, we fix the pulse energy at 200 nJ and the polarisation to circular.

2.3 Aberration compensation for fabricating optimal structures at depth

The laser focus becomes highly aberrated when positioned deep inside the substrate. This is due to the refractive index mismatch[20] at the interface between the air and the fused silica substrate. The dominant aberration is primary spherical, which can be described using the Z_4^0 Zernike polynomial. To investigate how this aberration can be corrected, microchannels were inscribed into a 2.0 mm thick fused silica substrate using SLM phase masks of half-unit Z_4^0 amplitude coefficients ranging from +1 to -11. For each phase mask, one microchannel was inscribed at 15 different depths spanning from 50 to 1730 µm. Figure 2(b) shows a linear relationship between the optimal Z_4^0 coefficients (c_1) and the writing depth (D). At a depth of 1.0 mm, the etching rate is 85% of the shallow one and remains higher than $400\,\mathrm{\mu m\,h^{-1}}$, sufficient for our purpose. Investigation of secondary spherical aberration (Z_6^0) was not found to result in any significant improvement. In this work, we use the linear relationship $c_1 = -0.005313D + 0.4948$ for continuous spherical aberration correction (Fig. 2(b)).

When inscribing with a high numerical aperture, the refractive index ratio does not perfectly predict the longitudinal focal volume shift when focussing into the substrate.[20] An experimental channel study confirmed

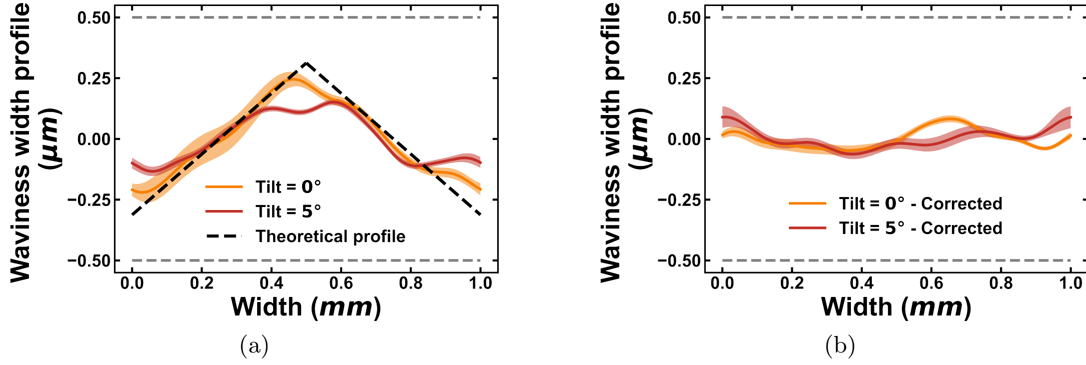

Figure 3. (a) Waviness width profile of a surface with no tilt (orange) and tilt = 5° (red). It is dominated by a triangular profile formed as the etchant propagates across the modified surface. We can fit it (dashed line) using the etching rate of pristine[16] and modified material. (b) Surfaces (0° and 5°) after a corrected inscription. The triangular profile is successfully removed. For (a) and (b), the profile mean value is shown with a shaded area corresponding to the standard deviation. The grey-dashed lines indicate the initial 1 µm target for the waviness.

the correction $s = 1.524478$ that will be used for the slice fabrication.[21] The longitudinal separation between consecutive laser scans is optimised to minimise writing time while preserving high etching rates. When using a pulse energy of 200 nJ, the optimal vertical separation was set at 6 µm.

3. SLICE FABRICATION

3.1 Fabrication description

We inscribed a $8 \times 5 \times 1$ mm rectangle in a $10 \times 10 \times 1$ mm fused silica substrate. For our purposes, the laser inscription always started with deeper structures such that the laser beam is not affected by previously modified regions. The inscription time is around 20 minutes, which is short enough to maximise laboratory and setup stability. Tilted surfaces, *i.e.* rotation along the x-axis in Fig 1, are inscribed using the same writing parameters up to 5°. In this case, only one 8×1 mm rectangle side is tilted, with the horizontal pivot axis located at 0.5 mm depth.

3.2 Waviness and roughness results

The topography of the surfaces is measured with an optical 3D-measurement system (Bruker Alicona, Focus-Variation). The roughness (S_q) is defined as the standard deviation of the measured surface after applying a high-pass filter with a cut-off frequency of $\lambda_c = 100$ µm. A low-pass filter with the same cut-off frequency is applied to the original data to obtain the waviness, which is defined as the mean difference between the five highest peaks and five deepest valleys (S_{10z}).

The roughness is pulse energy and tilt dependent. We measured $S_q = 109$ nm RMS and $S_q = 204$ nm RMS for surfaces with tilt of 0° and 5°, respectively. Figure 3(a) shows the waviness width profile for a flat surface with 0° tilt and 5° tilt. It is dominated by a triangular shape formed when the etchant attacks the pristine material while propagating through the modified plane. Unless accounted for, this will limit the precision with which freeform optics can be fabricated. However, the consistency of the ULAE process enables its correction. We fit the experimental profiles using[16] $\mathrm{ER}_{\mathrm{pristine}} = 0.5\,\mu\mathrm{m\,h^{-1}}$ and $\mathrm{ER}_{\mathrm{modified}} = 400\,\mu\mathrm{m\,h^{-1}}$. We inscribed the same two surfaces (0° and 5°) with a negative theoretical triangular profile. The waviness width profile of these surfaces after etching is shown in Fig. 3(b). The waviness was successfully reduced to $S_{10z} = 0.158$ µm. It is clear that the dominant triangular shape is eliminated after corrected inscription. In addition, Fig. 4 displays the 2D maps of the four surfaces previously described and highlights the superior flatness of the corrected ones. The waviness is well below the specified requirements, demonstrating that ULAE can manufacture 3D-structures with precise control of the surfaces.

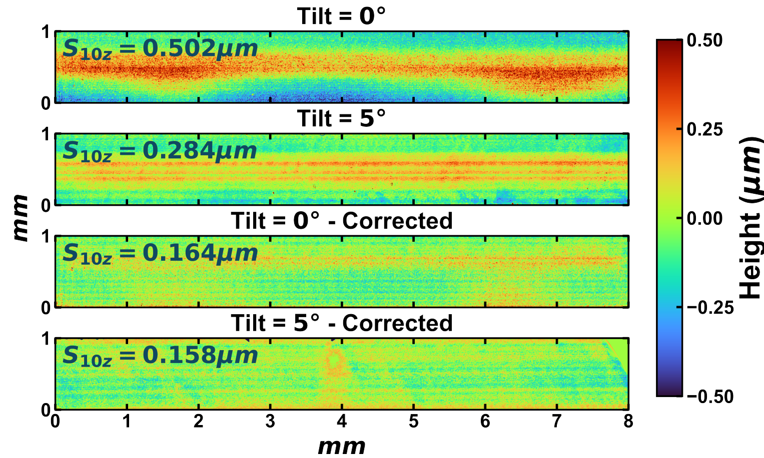

Figure 4. 2D-maps of the four surfaces described in Fig. 3. S_{10z} parameter for non-corrected and corrected ULAE manufactured surfaces highlights the quality of the corrected surface.

4. CONCLUSIONS

We demonstrate the fabrication of 8×1 mm fused silica surfaces with a waviness $S_{10z} = 0.158$ μm and a roughness $S_q < 204$ nm RMS. The roughness decreases to $S_q = 109$ nm RMS in case of surfaces tilted $\ll 1°$, as required for some image slicers designs. Combined with a suitable polishing technique such as CO_2 laser polishing, it may be possible to reduce the roughness to a few nanometres RMS.[17] Although we have only considered flat surfaces in this study, it is straightforward to create free-form surfaces using ULAE. We conclude that ULAE-manufactured optics may be able to meet the stringent requirements for elements such as image slicers at visible wavelengths and shorter.

ACKNOWLEDGMENTS

T.V.G. acknowledges support from Heriot-Watt University in the form of a James Watt Ph.D. scholarship. R.R.T. acknowledges support from the UK Science and Technology Facilities Council (STFC – Grant Number ST/V000403/1). We thank Light Conversion for their support.

REFERENCES

[1] Bowen, I., "The Image-Slicer a Device for Reducing Loss of Light at Slit of Stellar Spectrograph," *ApJ* **88**, 113 (1938).

[2] Wells, M., Lee, D., Oudenhuysen, A., Hastings, P., Pel, J.-W., and Glasse, A., "The MIRI medium resolution spectrometer for the James Webb Space Telescope," *Proc. SPIE* **6265**, 626514 (2006).

[3] Tajitsu, A., Aoki, W., and Yamamuro, T., "Image Slicer for the Subaru Telescope High Dispersion Spectrograph," *PASJ* **64**, 77 (2012).

[4] Ren, D. and Ge, J., "An Image Slicer Integral Field Unit with Diffraction-limited Performance for Three-Dimensional Imaging Spectroscopy," *PASP* **116**, 46–54 (2004).

[5] Tecza, M., Barnsley, R. M., Sukegawa, T., and Menduina-Fernandez, A., "Design and proto-typing of integral field units for the ELT-PCS test bench spectrograph," in [*Advances in Optical and Mechanical Technologies for Telescopes and Instrumentation III*], Geyl, R. and Navarro, R., eds., **10706**, 88, SPIE (2018).

[6] Laurent, F., Renault, E., Bacon, R., Dubois, J.-P., Hénault, F., and Robert, D., "Optical design, manufacturing, and tests of the MUSE image slicer," in [*Optical Fabrication, Testing, and Metrology II*], **5965**, 59650J, SPIE (2005).

[7] Bacon, R., Brinchmann, J., Richard, J., Contini, T., Drake, A., Franx, M., Tacchella, S., Vernet, J., Wisotzki, L., Blaizot, J., Bouché, N., Bouwens, R., Cantalupo, S., Carollo, C. M., Carton, D., Caruana, J., Clément, B., Dreizler, S., Epinat, B., Guiderdoni, B., Herenz, C., Husser, T.-O., Kamann, S., Kerutt, J., Kollatschny, W., Krajnovic, D., Lilly, S., Martinsson, T., Michel-Dansac, L., Patricio, V., Schaye, J., Shirazi, M., Soto, K., Soucail, G., Steinmetz, M., Urrutia, T., Weilbacher, P., and de Zeeuw, T., "The MUSE 3D view of the *Hubble* Deep Field South," *A&A* **575**, A75 (2015).

[8] Giesers, B., Dreizler, S., Husser, T.-O., Kamann, S., Escudé, G. A., Brinchmann, J., Carollo, C. M., Roth, M. M., Weilbacher, P. M., and Wisotzki, L., "A detached stellar-mass black hole candidate in the globular cluster NGC 3201," *MNRAS* **475**, L15–L19 (2018).

[9] Laurent, F., Renault, E., Kosmalski, J., Adjali, L., Boudon, D., Bacon, R., Caillier, P., Remillieux, A., Salaun, Y., and Delabre, B., "Muse image slicer: test results on largest slicer ever manufactured," in [*Advanced Optical and Mechanical Technologies in Telescopes and Instrumentation*], Atad-Ettedgui, E. and Lemke, D., eds., **7018**, 70180J, SPIE (2008).

[10] Thomson, R. R., Birks, T. A., Leon-Saval, S. G., Kar, A. K., and Bland-Hawthorn, J., "Ultrafast laser inscription of an integrated photonic lantern," *Opt. Express* **19**, 5698–5705 (2011).

[11] Thomson, R. R., Harris, R. J., Birks, T. A., Brown, G., Allington-Smith, J., and Bland-Hawthorn, J., "Ultrafast laser inscription of a 121-waveguide fan-out for astrophotonics," *Opt. Lett.* **37**, 2331–2333 (2012).

[12] Ross, C. A., MacLachlan, D. G., Choudhury, D., and Thomson, R. R., "Optimisation of ultrafast laser assisted etching in fused silica," *Opt. Express* **26**, 24343 (2018).

[13] Anagnos, T., Harris, R. J., Corrigan, M. K., Reeves, A. P., Townson, M. J., MacLachlan, D. G., Thomson, R. R., Morris, T. J., Schwab, C., and Quirrenbach, A., "Simulation and optimisation of an astrophotonic reformatter," *MNRAS* **478**(4), 4881–4889 (2018).

[14] McArthur, S. R., Thomson, R. R., and Ross, C. A., "Investigating focus elongation using a spatial light modulator for high-throughput ultrafast-laser-induced selective etching in fused silica," *Opt. Express* **30**, 18903 (2022).

[15] Ross, C. A., Harrington, K., Mears, R., Stone, J. M., Birks, T. A., and Thomson, R. R., "Axi-Stack: a method for manufacturing freeform air-silica optical fibre," *Opt. Express* **32**, 922 (2024).

[16] Casamenti, E., Pollonghini, S., and Bellouard, Y., "Few pulses femtosecond laser exposure for high efficiency 3D glass micromachining," *Opt. Express* **29**, 35054 (2021).

[17] Zhao, L., Cheng, J., Chen, M., Yuan, X., Liao, W., Liu, Q., Yang, H., and Wang, H., "Formation mechanism of a smooth, defect-free surface of fused silica optics using rapid CO_2 laser polishing," *IJEM* **1**, 035001 (2019).

[18] Shimotsuma, Y., Kazansky, P. G., Qiu, J., and Hirao, K., "Self-Organized Nanogratings in Glass Irradiated by Ultrashort Light Pulses," *PRL* **91**, 247405 (2003).

[19] Ochoa, M., Roldán-Varona, P., Algorri, J. F., López-Higuera, J. M., and Rodríguez-Cobo, L., "Polarisation-independent ultrafast laser selective etching processing in fused silica," *Lab Chip* **23**, 1752–1757 (2023).

[20] Salter, P. S., Baum, M., Alexeev, I., Schmidt, M., and Booth, M. J., "Exploring the depth range for three-dimensional laser machining with aberration correction," *Opt. Express* **22**, 17644 (2014).

[21] Cumming, B. P., Turner, M. D., Schröder-Turk, G. E., Debbarma, S., Luther-Davies, B., and Gu, M., "Adaptive optics enhanced direct laser writing of high refractive index gyroid photonic crystals in chalcogenide glass," *Opt. Express* **22**, 689 (2014).